AppliedChem

MDPI

Article

Exploring the Potential of *Cupriavidus metallidurans* and *Ochrobactrum anthropi* for ^{241}Am Bioaccumulation in Aqueous Solution

Leandro Goulart de Araujo [1,*], Tania Regina de Borba [1], Rafael Luan Sehn Canevesi [2], Sabine Neusatz Guilhen [1], Edson Antonio da Silva [2] and Júlio Takehiro Marumo [1]

[1] Instituto de Pesquisas Energéticas e Nucleares, Av. Prof. Lineu Prestes, São Paulo 05508-000, Brazil; trborba@hotmail.com (T.R.d.B.); snguilhen@ipen.br (S.N.G.); jtmarumo@ipen.br (J.T.M.)

[2] Centro de Engenharias e Ciências Exatas, Universidade Estadual do Oeste do Paraná, 645 Rua da Faculdade, Toledo 85903-000, Brazil; rafael_canevesi@hotmail.com (R.L.S.C.); edsondeq@hotmail.com (E.A.d.S.)

* Correspondence: lgoulart@alumni.usp.br

Abstract

This study explores, for the first time, the bioaccumulation of americium-241 (^{241}Am) by *Cupriavidus metallidurans* and *Ochrobactrum anthropi*, two bacterial strains previously investigated mainly for their interactions with other heavy metals and radionuclides. To the best of our knowledge, no prior studies have reported the use of these microorganisms for ^{241}Am removal from aqueous solutions. The effects of initial ^{241}Am concentration and solution pH on removal performance were evaluated through batch experiments. Kinetic analyses were performed using pseudo-first-order (PFO) and pseudo-second-order (PSO) models, with the PSO model providing a better fit, suggesting chemisorption as the rate-limiting step in the process. Initial ^{241}Am concentrations ranged from 75 to 300 Bq mL^{-1}, and both bacterial strains demonstrated comparable maximum bioaccumulation capacities of approximately 1.5 × 10^{-8} mmol g^{-1}. However, *O. anthropi* exhibited superior resistance to ^{241}Am, maintaining colony growth at activity levels up to 1200 Bq mL^{-1}, compared to a threshold of 400 Bq mL^{-1} for *C. metallidurans*. These findings highlight the robustness and efficiency of these bacterial strains—particularly *O. anthropic*—in removing ^{241}Am from liquid radioactive waste, offering promising implications for bioremediation technologies.

Keywords: americium-241; bacterial strains; adsorption; radioactive liquid waste

check for updates

Academic Editor: Jason Love

Received: 25 July 2025
Revised: 14 October 2025
Accepted: 6 November 2025
Published: 11 November 2025

Citation: de Araujo, L.G.; de Borba, T.R.; Canevesi, R.L.S.; Guilhen, S.N.; da Silva, E.A.; Marumo, J.T. Exploring the Potential of *Cupriavidus metallidurans* and *Ochrobactrum anthropi* for ^{241}Am Bioaccumulation in Aqueous Solution. *AppliedChem* **2025**, *5*, 34. https://doi.org/10.3390/appliedchem5040034

Copyright: © 2025 by the authors. Licensee MDPI, Basel, Switzerland. This article is an open access article distributed under the terms and conditions of the Creative Commons Attribution (CC BY) license (https://creativecommons.org/licenses/by/4.0/).

1. Introduction

The transuranic artificial radionuclide ^{241}Am (432.2 years of half-life) is commonly found in devices such as lightning rods, smoke detectors, and various applications within the nuclear industry. It is also frequently detected in liquid radioactive waste generated by nuclear research activities. ^{241}Am is one of the most hazardous contaminants due to its high radiotoxicity and long half-life. It decays by alpha emission to ^{237}Np and, when absorbed by the human body, it tends to accumulate in the bones and liver, potentially inducing malignant tumors [1]. The committed effective dose coefficients are tabulated in ICRP Publication 119, which defines safety reference values for radionuclide intake by workers and the general public [2]. The maximum permissible body burden for ^{241}Am is 11.1 kBq (approximately 8.76 × 10^{-8} g), and the drinking water limit is 1.48 Bq mL^{-1} (1.17 × 10^{-6} g L^{-1}) [3]. The U.S. EPA also limits total alpha-emitting radionuclides (in-

cluding americium) to 15 pCi L^{-1} (≈0.555 Bq L^{-1}), in drinking water under the National Primary Drinking Water Regulations [4].

In aqueous environments, americium exists predominantly as Am^{3+}, a trivalent actinide ion with a relatively large ionic radius (0.982 Å), high hydration energy (7.4–10 Å), and strong affinity for ligands such as phosphate, carbonate, and carboxylate groups [5–7]. These properties govern its mobility and reactivity in natural and engineered systems. Despite its environmental relevance, the removal of Am^{3+} remains a significant challenge due to its stable oxidation state and strong complexation behavior [8]. Although conventional methods—such as precipitation, ion exchange, and electrochemical processes—have been employed, the large volumes of contaminated solutions and the typically low concentrations of americium ions render these methods inefficient [9].

Advanced partitioning techniques, including TALSPEAK [10], DIAMEX/SANEX (Diamide Extraction/Selective Actinide Extraction) [11], and PUREX (Plutonium Uranium Reduction Extraction) [12], have been developed for effective actinide separation. However, these approaches require highly specialized infrastructure and involve extensive processing steps, such as nitric acid dissolution of nuclear fuel, multi-stage solvent extraction cycles, robust containment systems, and stringent safety and proliferation controls [13].

Recent research has increasingly turned toward innovative techniques for radionuclide removal, with particular attention given to bioaccumulation processes. Bioaccumulation involves the uptake of metals by living biomass, such as microbial cells or tissues [14], and relies on the inherent capacity of the biomass to bind, absorb, or adsorb metal ions from aqueous solutions [15].

In bioaccumulation mechanisms, many microorganisms effectively bind to hazardous and potentially toxic metal ions. Two primary mechanisms of metal ion removal are recognized. The first involves binding at the cell membrane surface, which occurs without energy expenditure. In the second, metal ions cross the cell membrane and participate in intracellular biochemical pathways. The surface binding of metal ions is particularly significant and often represents the primary method of metal ion removal [16].

Metal binding is facilitated by the abundance of functional groups on cell membranes, which are primarily composed of proteins, lipids, and polysaccharides. These groups include carboxylates, amines, amides, hydroxyls, phosphates, thiols, and others, all of which provide sites for metal ion attachment [15,17].

The cell wall acts as a complex ion exchanger, comparable to a resin. Its ion exchange capacity depends on the presence of functional groups and the spatial structure of the wall itself. Key functional groups responsible for metal uptake include carboxyl, amino, sulfate, and phosphate groups. These facilitate the capture of metal cations through electrostatic attraction or dipole-dipole interactions. This interaction is particularly pronounced in the case of metal ions due to the anionic characteristics of the cell wall [18,19].

The use of living, resistant microbial biomass presents a promising alternative to the detoxification of industrial hazardous effluents, contributing to environmental protection and the recovery of valuable metals. For instance, living biomass (*P. aeruginosa*) has already demonstrated a 40% improvement in lead removal compared to its inactivated form [20].

A review of the extant literature reveals numerous studies addressing the removal of radionuclides from aqueous solutions using biologically derived materials. For instance, tannin has been examined for its capacity to extract U(VI)/Th(IV) [21], calcium alginate aerogels for ^{232}U and ^{241}Am [22], *Saccharomyces cerevisiae* for U/Sr [23,24], *Aspergillus niger* for ^{85}Sr and ^{99m}Tc [25], and *Candida utilis* for its ability to remove U(VI) [26]. These investigations have examined the potential of these materials to remove americium from solutions. Among microbial species, *Cupriavidus metallidurans* (*C. metallidurans*), a Gram-negative, non-pathogenic, β-proteobacterium, has garnered attention for its exceptional resistance

to heavy metals [27,28]. *Cupriavidus* (ex *Ralstonia*) *metallidurans* CH34 is a hydrophobic, metal-resistant bacterium isolated from the sludge of a zinc decantation tank in Belgium, which was contaminated with high concentrations of several heavy metals [27]. This bacterium has gained increasing interest as a model organism for the study of heavy metal detoxification and biotechnological applications.

Despite the well-documented resistance of *C. metallidurans* to various transition metals, its interaction with actinides such as americium remains largely unexplored. *C. metallidurans* is well known for its heavy metal detoxification capabilities, conferred by multiple resistance determinants. These include Resistance-Nodulation-Division (RND) family efflux systems and a variety of metal resistance operons located on its two megaplasmids, pMOL28 and pMOL30 [29–31].

The evolution of *C. metallidurans* as a metal-resistant bacterium is well described in the literature [29]. The authors mention that the cobalt–nickel and chromate resistance determinants located on pMOL28 are believed to have evolved through gene duplication and horizontal gene transfer, promoting adaptation to metal-rich environments such as serpentine soils. On pMOL30, the *czc* (cobalt-zinc-cadmium) resistance operon coexists with resistance genes for copper, lead, and mercury. The *czc* determinant likely originated from the duplication of a chromosomal *czcICBA* core cluster (located on chromosome 2), which was further extended by the addition of upstream *czcN* and downstream genes and efflux genes of *czcICBA* (*czcD*, *czcRS*, *czcE*) [29].

Altogether, *C. metallidurans* appears to have evolved its exceptional metal resistance through a combination of horizontal gene acquisition and operon duplication, particularly targeting genes related to transition metal efflux. This genomic architecture is further complemented by a reduced repertoire of metal uptake systems, minimizing intracellular accumulation of toxic ions [30,32]. However, the unique speciation and coordination behavior of trivalent actinides such as $^{241}Am^{3+}$ may pose challenges to these classical detoxification systems, since actinides differ significantly in ionic radius and complexation behavior compared to transition metals [33]. Meanwhile, although *Ochrobactrum anthropi* (*O. anthropic*) has been described as metal-tolerant and isolated from contaminated environments [34], we are unaware of studies evaluating its resistance to actinides or other radionuclides.

Monthy et al. [27] also demonstrated that, depending on the metal, it may concentrate in different regions of *C. metallidurans* plasmid pMOL28. This difference may result in distinct bioaccumulation behaviors depending on the contaminant. Studies have demonstrated that *C. metallidurans* already presents high resistance to a large variety of metals. Some examples are lead [35], molybdenum and vanadium [36], platinum [37], zinc [38], mercury and lead [39], cadmium [40], and uranium [41].

The bacterium *O. anthropi* is a Gram-negative bacillus, classified as *Achromobacter*, and currently recognized as belonging to the genus *Ochrobactrum*. This organism has a broad environmental distribution, being found in water, soil, plants, among other environments. *Ochrobactrum* strains are of particular interest for bioremediation. They can degrade organophosphorus pesticides, toxic solvents, petroleum residues, and are also capable of removing chromium, cadmium, copper, and other toxic metals from the environment [42–44]. Li et al. [45] reported a 95% removal efficiency for Cr(IV) by *O. anthropi* at an initial concentration of 400 mg L^{-1}. De Pádua Ferreira et al. [46] found *O. anthropi* in slurry samples from lysimeters containing ^{241}Am and suggesting its potential resistance to this radionuclide and its applicability in removing americium from radioactive waste.

Given their biological and biochemical attributes, *C. metallidurans* and *O. anthropi* offer promising features for the biotechnological removal of radionuclides. *C. metallidurans* harbors a complex network of metal-resistance operons (e.g., *czc*, *cop*, and *cnr*) distributed

across two large megaplasmids (pMOL28 and pMOL30), enabling efficient detoxification of heavy metals via efflux pumps, oxidative stress responses, and reduced uptake mechanisms [47,48]. This strain has already demonstrated resistance to a wide range of metals, including Pb, Mo, V, Zn, Hg, Cd, and U [31,36,49–51]. Genomic adaptations such as operon duplication and horizontal gene transfer have further enhanced its resilience in metal-rich environments such as serpentine soils or industrial effluents [29,52].

While *O. anthropi* is less studied in the context of radionuclides, it has been frequently isolated from contaminated environments and is known to form biofilms and secrete exopolysaccharides, facilitating the sorption of Cr, Cu, Cd, and other heavy metals [43,53,54]. It has also demonstrated the capacity to degrade xenobiotics such as organophosphates and petroleum residues, reinforcing its value for environmental bioremediation [55,56]. Notably, it has been detected in lysimeters containing ^{241}Am, suggesting a potential tolerance to actinides [46].

Despite these promising traits, the potential of *C. metallidurans* and *O. anthropi* for the bioaccumulation of actinides, particularly trivalent species like Am^{3+}, remains largely unexplored. This study aims to evaluate, for the first time, the capacity of metabolically active cells of these strains to uptake ^{241}Am in aqueous solution, as well as their radiotolerance. Batch experiments were carried out at three initial activity concentrations and multiple contact times, and minimum inhibitory concentration (MIC) assays were conducted over a wide range of ^{241}Am levels. In this context, the term *bioaccumulation* refers to the net uptake of ^{241}Am by living, active cells under aqueous conditions, without fixation or inactivation steps. While this includes surface adsorption and potentially intracellular processes, the specific contribution of each was not independently quantified. These findings provide foundational data for the future development of biologically based and cost-effective strategies for the remediation of liquid radioactive waste containing trivalent actinides.

2. Materials and Methods

2.1. Bacteria Preparation

C. metallidurans and *O. anthropi* were selected for the bioaccumulation experiments. *C. metallidurans* was supplied by the Institute of Biosciences of the University of São Paulo. The strain grew under aerobic conditions in nutrient broth (NB) at 28 °C, following standard protocols [57]. *O. anthropi*, isolated from the manure collected from lysimeters in prior studies [46], was cultured in brain heart infusion medium (Difco, BD Diagnostics, Sparks, MD, USA) for 24 h in an oven at 37 °C under constant stirring. Before the bioaccumulation experiments, the following analyses were performed: bacterial growth curve, MIC, and cell viability for 50% lethal dose (LD50).

MIC studies were undertaken for the two bacteria to determine the minimum ^{241}Am amount capable of inhibiting the growth of microorganisms, using a successive dilution method [58]. All MIC experiments were plated in triplicate. Bacterial biomass was obtained by growing cells in Tris Salt Medium (TSM) with subsequent addition of ^{241}Am. TSM was prepared according to the formulation described in [34] and consisted of the following components: Tris-HCl (50 mmol L^{-1}), NaCl (80 mmol L^{-1}), $MgCl_2$ (2 mmol L^{-1}), $CaCl_2$ (0.27 mmol L^{-1}), KCl (20 mmol L^{-1}), and glucose (10 g L^{-1}). The final pH was adjusted to 7.0 for *O. anthropi* and 5.0 for *C. metallidurans* using HCl or NaOH solutions as needed. The estimated total ionic strength of the medium, assuming full dissociation of salts, was approximately 0.138 mol L^{-1}. Details of the ionic strength calculation and the total medium composition are provided in the Supplementary Materials (Text S1 and Tables S1–S3, respectively).

All experiments were conducted in TSM, with consistent composition and pH conditions applied separately for each bacterial strain. This ensured that any potential back-

ground interactions between americium and the medium components remained constant within each experimental set. The medium contains defined amounts of inorganic salts and low concentrations of organic components, without any chelating agents, minimizing the likelihood of strong complexation with Am^{3+}. Moreover, no visual signs of turbidity, precipitation, or colloid formation were observed in the control tubes during the course of the experiments. Centrifugation was performed before radiometric analysis, and only the clear supernatant was measured, further reducing the risk of interference from non-biological retention. These precautions support the conclusion that the observed differences in americium uptake can be attributed to the presence and activity of the bacterial biomass.

Americium solution was purchased from Amersham, England. Activities of the synthetic solutions were 20, 40, 80, 120, 150, 175, 200, 225, 250, 300, 350, 400, 450, 800, 1000, 1200, 1400, 1800, and 2000 Bq mL^{-1}. These solutions were prepared from a stock solution of 2450.50 Bq mL^{-1} Americium chloride ($AmCl_3$). The tolerance ranges studied for $AmCl_3$ were 7×10^{-4} to 6×10^{-2} µmol L^{-1} (Bq mL^{-1}). Homogeneity of ^{241}Am in the aqueous medium was maintained by constant stirring (90 rpm) during sample preparation and incubation. Although data on the exact solubility of $AmCl_3$ in pure water are limited, americium(III) compounds are generally considered highly soluble under neutral conditions [59,60]. Additionally, all experimental conditions were prepared identically using calibrated micropipettes to dispense appropriate aliquots per flask, thereby ensuring uniform exposure. All procedures involving ^{241}Am were conducted in a licensed radiological facility following strict safety protocols, including the use of HEPA-filtered fume hoods, personal protective equipment, and dosimetry monitoring, in accordance with institutional and regulatory guidelines for handling alpha-emitting radionuclides.

An aliquot of 50 mL from each culture was centrifuged at 2500 rpm for 15 min, and the supernatant was discarded. Pellets were washed and resuspended in TSM. This procedure was performed thrice to eliminate the culture medium. The optical density (OD) of the bacterial suspension in the TSM was adjusted to 1 at 600 nm. In pre-autoclaved 22 mL quartz flasks, 9 mL TSM were combined with 1 mL of TSM containing bacteria. Serial dilutions up to 10^{-8} were prepared, according to the National Committee for Clinical Laboratory Standards [58]. These samples were incubated at 37 °C under constant agitation for 24 h before plating

Growth curve studies for each bacterial strain were conducted in triplicate. After inoculation, the OD at 600 nm (OD600) was measured hourly for 10 h [61]. For the flow cytometry assays, 200 µL of each bacterial suspension at OD600 was added to individual tubes. Three controls were prepared (one for each strain), and for each sample, two tubes were set up: one with Triton, to permeabilize the cell wall and ensure membrane permeability, and one without Triton. To each tube, 10 µL of propidium iodide (18 µg mL^{-1}) was added, followed by agitation and incubation for 30 min. Then, 1 mL of FACS Flow buffer was added, and the samples were centrifuged for 15 min at 2000 rpm. Supernatants were discarded, and the pellets were resuspended in 200 µL of FACS Flow buffer plus 10 µL of 1% paraformaldehyde. After gentle mixing, the samples were placed on crushed ice in a closed Styrofoam box wrapped in aluminum foil. From each prepared solution, 1.2 mL was taken, supplemented with 60 µL of Rhodamine 123, and then analyzed in a FACScalibur flow cytometer (Becton-Dickinson, San Jose, CA, USA), as previously described [62].

Rhodamine 123 is a cationic fluorochrome that selectively accumulates in cells with polarized membranes, serving as a marker for metabolic activity and viability. Approximately 10,000 events were recorded per sample, and data were processed using CellQuest software (version 5.2.1). Debris was excluded based on forward and side scatter (FSC/SSC) profiles. Viability gates were established by comparing fluorescence profiles of untreated controls and Am-exposed cultures, assuming that low FL-1 intensity corresponds to depolarized,

metabolically inactive cells. Although no chemically inactivated positive control was used, visual inspection of the bimodal fluorescence distribution enabled consistent separation of viable and non-viable populations.

All glassware and quartz flasks were autoclaved prior to use. Bacterial manipulations were performed using sterile pipettes, tips, and gloves, inside a laminar flow hood. Culture purity was verified by streaking aliquots of each strain on nutrient agar plates and confirming colony morphology consistency. No contamination was observed throughout the experiments. After OD600 adjustment to 1.0, cell suspensions were serially diluted and plated to quantify CFU mL^{-1}, ensuring comparable concentrations of viable cells between strains. Flow cytometry with Rhodamine 123 staining was additionally used to confirm cell viability and metabolic activity prior to exposure to ^{241}Am solutions.

2.2. Americium Uptake Experiments

Aliquots of each bacterial culture were centrifuged at 2500 rpm for 15 min. The supernatant was discarded, and the pellets were resuspended in TSM at pH 7 for *O. anthropi* and pH 5 for *C. metallidurans*. Resuspended solutions were then centrifuged at 2500 rpm for 15 min twice to remove the culture medium. The adjustment of OD was made to 2.5, corresponding to a bacterial mass of approximately 2 mg. ^{241}Am solutions were prepared in TSM at pH 7 and 5, at concentrations of 150, 300, and 600 Bq mL^{-1}.

The bioaccumulation/biosorption experiments were performed in triplicate using batch mode using 1.5 mL TSM solution containing ^{241}Am and 1.5 mL TSM containing bacteria. As a result, the ^{241}Am initial concentrations were 75, 150, and 300 Bq mL^{-1} (2.45×10^{-9}, 4.90×10^{-9}, and 9.80×10^{-9} mmol L^{-1}, respectively). The solutions were placed into 22 mL capacity quartz flasks under sterile conditions. The vials were packed in plastic bags, placed in polyethylene bottles, and maintained under constant stirring at room temperature for different contact times, depending on the bacteria. The contact times tested were 1, 2, 4, 6, 12, and 24 h for *C. metallidurans* and 0.03, 0.08, 0.5, 1, 2, 4, 6, 12, 24 h for *O. anthropi*.

After incubation at each designated contact time, the solutions were centrifuged at 2500 rpm for 15 min, and 1 mL of the supernatant was collected for scintillation analysis. The method used is described by Li et al. [45], and allowed the detection of residual activity concentrations of americium. The measurements were performed by comparison with a reference standard from Amersham International (GE Healthcare, Amersham, Buckinghamshire, UK), with an activity/mass of 785.823 kBq g^{-1}. One milliliter of the prepared solution was mixed with 19 mL of scintillator liquid inside 22 mL quartz flasks [63]. The sample was vortexed for 1 min and placed in the scintillator for 30 min. The residual americium was quantified in a Tri-Carb 2100 TR Liquid Scintillation Analyzer (Packard-Canberra, Meriden, CT, USA). The dry mass was determined by subjecting the adsorbent post-treatment to a drying process in an oven (WTC Binder, Tuttlingen, Germany) maintained at 80 °C for a period of 4 h.

2.3. Americium Removal and Kinetics

The amount of americium was calculated from the difference in the americium concentration in the aqueous solution before and after bioaccumulation. The kinetic study considered the americium uptake by the following equation:

$$q = (Ci - Cf)\, V/m \quad (1)$$

where q is the concentration of americium in the bacteria (mmol g^{-1}), C_i and C_f are the initial and the final ^{241}Am concentration in solution (mmol L^{-1}), V is the solution volume (L) and m is the initial mass of bacteria (g).

Bioaccumulation rate has been described by several kinetic model approaches, in batch operations, as a function of solution concentrations with different reaction orders or regarding the adsorbent capacity. There is also the consideration of the rate of population growth/decrease in the aqueous media in the removal of metals by living microorganisms. The determination of bioaccumulation kinetics is crucial to properly evaluate the removal efficiency of ^{241}Am and for the design of effluent treatment on an industrial scale.

In the models used, the population of bacteria was considered to remain constant during the kinetic experiment, since the rate of growth is slow when compared to the kinetic rate. Pseudo-first-order (PFO) kinetics is commonly applied to describe the biosorption/adsorption of metals using different types of biomasses. This model was described by the differential equation and is given as follows [64]:

$$dq/dt = k_1 (q_{eq} - q) \quad (2)$$

where q and q_{eq} are the concentration of americium in the bacteria over time and at the equilibrium, respectively; k_1 is the PFO rate constant.

Also, the mathematical equation for Pseudo-second-order (PSO) kinetics was proposed [65].

$$dq/dt = k_2 (q_{eq} - q)^2 \quad (3)$$

where k_2 is the PSO rate constant, q_{eq} is the concentration of americium in the bacteria at the equilibrium, and q is the amount of the solute adsorbed in time.

In this study, the PFO and PSO kinetics were applied in their nonlinear forms to evaluate all adsorbents' performance and to elucidate the mechanisms involved. The error metrics employed were the coefficient of determination (R^2), the Mean Absolute Error (MAE), and the Root Mean Squared Error (RMSE), with the corresponding equations provided in the Supplementary Materials (Text S2).

3. Results and Discussion

3.1. Preliminary Experiments

The growth curves of *O. anthropi* and *C. metallidurans* are presented in Figure 1, while the MIC results for the bioaccumulation experiments are summarized in Table 1. Although *O. anthropi* exhibited faster growth compared to *C. metallidurans*, both bacteria displayed similar growth patterns.

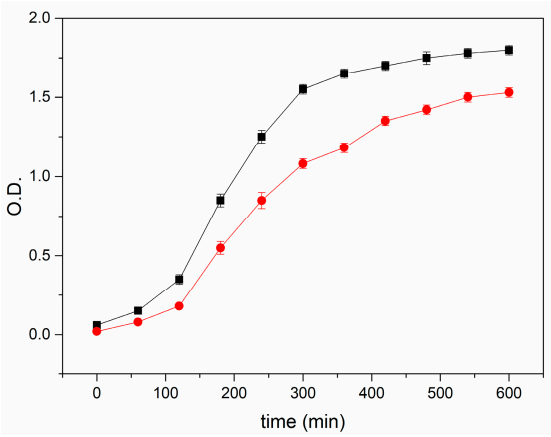

Figure 1. Growth curves of *Ochrobactrum anthropi* (black squares) and *Cupriavidus metallidurans* (red circles). Error bars represent the standard deviation from triplicate measurements.

Table 1. MIC ("+" growth of bacteria; "-" no growth of bacteria).

Activity Concentration (Bq mL^{-1})	Bacteria	
	C. metallidurans	*O. anthropi*
40	+	+
80	+	+
120	+	+
150	+	+
200	+	+
250	+	+
300	+	+
350	+	+
400	+	+
500	-	+
700	-	+
800	-	+
900	-	+
1000	-	+
1200	-	+
1400	-	-

Regarding their resistance to americium, *O. anthropi* presented superior tolerance, with colonies growing even at activity concentrations of up to 1200 Bq mL^{-1}, as shown in Table 1. This resilience can be attributed to prior exposure to ^{241}Am in the lysimeter from which it was isolated. Ferreira et al. [46] reported that bacterial consortia containing *O. anthropi* were four times more tolerant to $^{241}Am^{3+}$ than *Pseudomonas putida* F1. Conversely, *C. metallidurans* exhibited significantly lower resistance, with growth-restricted activity concentrations up to 400 Bq mL^{-1}.

The viability of bacterial cells after 5 h of exposure to americium at LD-50 (lethal dose for 50% of the population) is depicted in Figure 2. The LD-50 values determined by the flow cytometry technique were 200 Bq mL^{-1} for *C. metallidurans* and 600 Bq for *O. anthropi*.

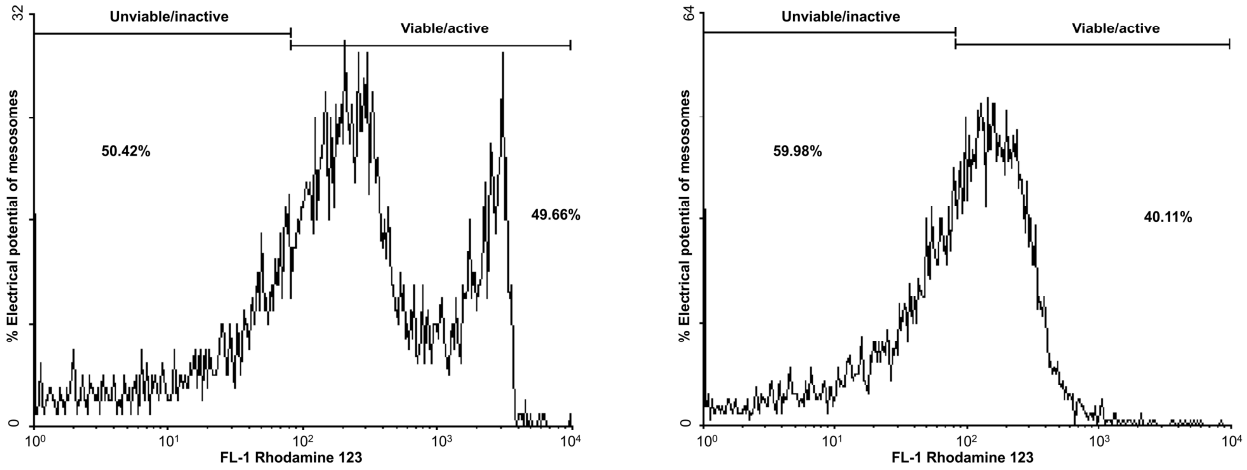

(**A**) (**B**)

Figure 2. Viability of the bacteria after 5 h of contact with ^{241}Am/LD-50. (**A**) *C. metallidurans*; (**B**) *O. anthropi*.

After 5 h of contact with 200 Bq ^{241}Am, 49.66% of *C. metallidurans* cells remained viable, as indicated in Figure 2A. For *O. anthropi*, 40.11% of cells remained viable after 5 h exposure to 600 Bq mL^{-1}, as shown in Figure 2B.

We recognize that flow cytometry data may be influenced by potential artifacts. For example, the presence of americium or other actinides could interfere with dye binding or fluorescence emission. In addition, cell aggregation may result in underestimation of total events, and autofluorescence of the bacterial cells can partially overlap with the signal of the viability dye. These limitations were minimized by including appropriate controls, using single-color staining, and applying strict gating strategies.

3.2. Uptake of ^{241}Am by Bacteria

The bioaccumulation results for *O. anthropi* and *C. metallidurans* at initial americium concentrations of 75, 150 and 300 Bq mL^{-1} are displayed in Figure 3.

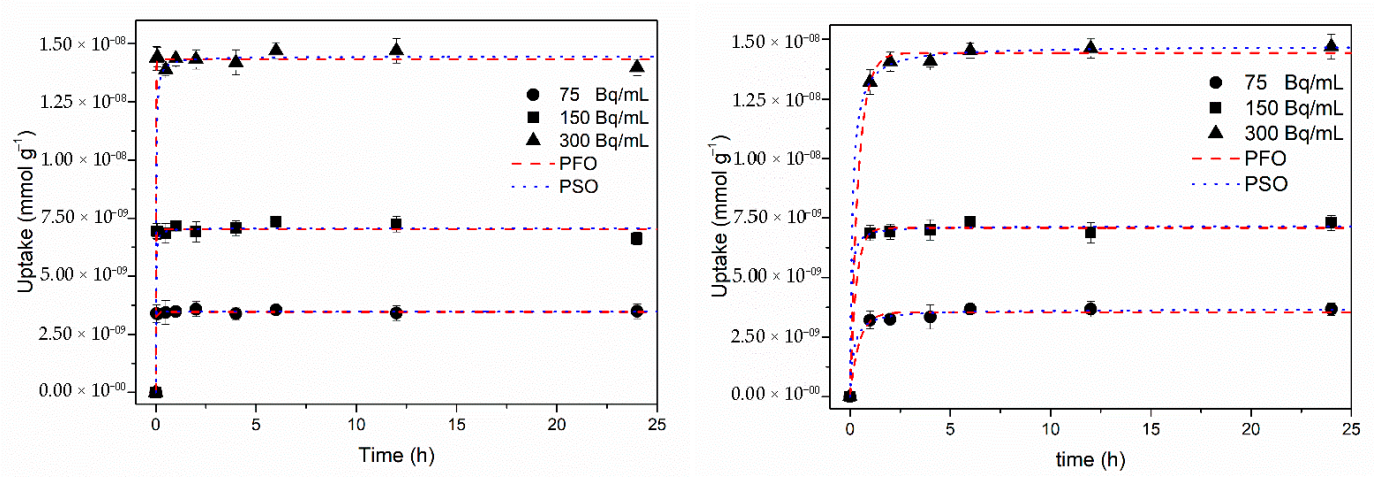

Figure 3. Bioaccumulation of americium, in the following initial activity concentrations: 75, 150, and 300 Bq mL^{-1}. (**A**) *O. anthropi*; (**B**) *C. metallidurans*.

The results indicate that higher americium concentrations led to increased bioaccumulation capacities. For *O. anthropi* (Figure 3A), equilibrium was reached at the very beginning for all initial americium concentrations, with no significant increase in bioaccumulation capacity even after 24 h. However, q (mmol g^{-1}) was remarkably superior with increased initial americium concentrations, reaching a maximum of 1.47×10^{-8} mmol g^{-1} ($[^{241}Am]_0$ = 300 Bq mL^{-1}). These values of q are comparable to those obtained by [46]. The authors used various bacterial communities to treat radioactive liquid organic waste. As concerns the removal of ^{241}Am, q values were 1.1×10^{-9} mmol g^{-1}, 5.4×10^{-10} mmol g^{-1}, and again 5.4×10^{-10} mmol g^{-1} for the three different bacterial communities. The values presented in this study surpass those reported by [46]. However, they employed bacterial communities to treat a complex radioactive waste, with the presence of other radionuclides such as cesium and uranium, which may have impaired higher bioaccumulation capacities by ionic competition.

The experiments with *O. anthropi* revealed to be efficient and a fast bioaccumulation process since an average removal of 95% was observed after 2 min of contact for all studied concentrations. The results achieved for *C. metallidurans* were very close to those obtained by *O. anthropi*. In terms of percentage removal, an average of 90% of the initial ^{241}Am activity concentration was removed in the 1 h contact. Furthermore, at 6 h of contact, an average of 99.6% of removal was reached for all activity concentrations of ^{241}Am.

The bioaccumulation performance observed in this study can be contextualized by comparing it with results from other biomaterials reported in the literature. Table 2 summarizes these values for various biomaterials tested for americium uptake, providing a comprehensive perspective on their biosorption and bioaccumulation capacities under

different conditions. This comparison highlights the potential of *O. anthropi* and *C. metallidurans* for the removal of ^{241}Am from aqueous solutions. The bioaccumulation performance observed in this study can be contextualized by comparing it with results from other biomaterials reported in the literature. As shown in Table 2, most of the reported studies focus on biosorption processes using inactivated biomass, such as *Rhizopus arrhizus*, *Saccharomyces cerevisiae*, or tannin-based materials, which typically achieve high removal efficiencies (95–99%) with contact times ranging from 60 to 200 min. In contrast, the present study demonstrates that live bacterial strains such as *O. anthropi* and *C. metallidurans* can achieve similarly high removal efficiencies (95–99.6%) but in much shorter time frames (as little as 2 to 60 min). These results reinforce the potential of active bioaccumulation for the efficient removal of americium from aqueous systems. Due to the scarcity of studies focusing specifically on the bioaccumulation of radionuclides, especially actinides like americium, the data presented here contribute valuable insights into this underexplored area, complementing the broader body of work on biosorption. The kinetic parameters for the PFO and PSO models are presented in Table 3.

Table 2. Comparison of biosorption/bioaccumulation capacities (q), removal efficiencies (R), and contact times for ^{241}Am uptake by various biomaterials reported in the literature.

Biomaterial	Adsorption Type	q_{max} or q_{eq} (mmol g^{-1})	R (%)	Contact Time	Reference
Tannin	Biosorption	7×10^{-3}	-	~200 min	[66]
Saccharomyces cerevisiae	Biosorption	-	95	60 min	[67]
Rhizopus arrhizus	Biosorption	-	99	60 min	[3]
Rhizopus arrhizus	Biosorption	-			[68]
Rhizopus arrhizus	Biosorption	-	97	120 min	[69]
Candida sp.	Biosorption	-	98	240 min	[70]
Pseudomonas fluorescens	Biosorption	-	100	-	[71]
Pseudomonas	Biosorption	-	72	-	[72]
Bacteria communities	Bioaccumulation	1.1×10^{-9} 5.4×10^{-10} 5.4×10^{-10}	-	-	[46]
Sepia officinalis (cuttlefish)	Bioaccumulation	-	65	-	[73]
Elodea canadensis	Bioaccumulation	2.6×10^{-5} *	-	-	[74]
Acipenser gueldenstaedtii (diamond sturgeon)	Bioaccumulation	-	50	14–28 days	[75]
O. anthropi	Bioaccumulation	1.47×10^{-8}	95	2 min	This study
C. metallidurans	Bioaccumulation	-	99.6	360 min	This study

* Maximum ^{241}Am activity concentration/specific alpha activity of ^{241}Am (1.27×10^{11} Bq mol^{-1}).

Table 3. Kinetic parameters of pseudo-first-order and pseudo-second-order models [a] for the bioaccumulation of ^{241}Am *O. anthropi*, and *C. metallidurans*.

			PFO				PSO		
Bacteria	**pH**	**C_0 (Bq mL^{-1})**	**$q_{eq,exp} \cdot 10^{-10}$ (mmol g^{-1})**	**k_1 (h^{-1})**	**$q_{eq,calc} \cdot 10^{-10}$ (mmol g^{-1})**	**R^2**	**$k_2 \times 10^2$ (g mmol^{-1} h^{-1})**	**$q_{eq,calc} \cdot 10^{-10}$ (mmol g^{-1})**	**R^2**
O. anthropi	7	75	34.93	119.76	34.64	0.996	3.04	34.73	0.997
	7	150	66.20	136.19	70.15	0.991	1.39	70.68	0.992
	7	300	139.74	466.16	143.33	0.997	0.42	144.48	0.998
C. metallidurans	5	75	36.73	2.22	35.41	0.986	0.16	36.67	0.994
	5	150	72.88	3.41	70.94	0.996	0.29	71.69	0.996
	5	300	146.94	2.43	144.30	0.998	0.06	147.26	1.000

[a] k_1 (h^{-1}) and k_2 (g mmol^{-1} h^{-1}) are the rate constants of the first and second order models, respectively.

Both the PFO and PSO models provided a good description of the experimental data for *O. anthropi* and *C. metallidurans*. The PFO rate constant (k_1) provides insights into

the speed of the process. This model is often applied to systems where physisorption dominates. However, as shown in Table 3, the R^2 for the PFO model were generally lower compared to the PSO model, suggesting that the americium bioaccumulation by both *O. anthropi* and *C. metallidurans* is not primarily governed by physisorption.

The PSO model is typically associated with chemisorption, where chemical bonding or electron sharing between the sorbate and the sorbent occurs. The kinetic parameter k_2 reflects the rate constant for chemisorption. As indicated in Table 3, the PSO model provided a better fit to the experimental data, with R^2 values exceeding 0.99 for most conditions. Therefore, it is hypothesized that the rate-limiting step was driven by chemisorption.

For *O. anthropi*, the PFO model yielded calculated equilibrium capacities ($q_{e,calc}$) of 34.64, 70.15, and 143.33 $\times$ 10^{-10} mmol g^{-1} at initial concentrations of 75, 150, and 300 Bq mL^{-1}, respectively, compared to the experimental values of 34.93, 66.20, and 139.74 $\times$ 10^{-10} mmol g^{-1}. This resulted in a MAE of 2.61 $\times$ 10^{-10} mmol g^{-1} and an RMSE of 3.09 $\times$ 10^{-10} mmol g^{-1}. In contrast, the PSO model produced $q_{e,calc}$ values of 34.73, 70.68, and 144.48 $\times$ 10^{-10} mmol g^{-1}, with a MAE of 3.14 $\times$ 10^{-10} mmol g^{-1} and an RMSE of 3.77 $\times 10^{-10}$ mmol g^{-1}.

For *C. metallidurans*, the PFO model gave $q_{e,calc}$ values of 35.41, 70.94, and 144.30 $\times$ 10^{-10} mmol g^{-1} at initial concentrations of 75, 150, and 300 Bq mL^{-1}, leading to a MAE of 1.97 $\times$ 10^{-10} mmol g^{-1} and an RMSE of 2.04 $\times$ 10^{-10} mmol g^{-1}, while the PSO model yielded $q_{e,calc}$ of 36.67, 71.69, and 147.26 $\times$ 10^{-10} mmol g^{-1}, with a MAE of 0.52 $\times$ 10^{-10} mmol g^{-1} and an RMSE of 0.71 $\times$ 10^{-10} mmol g^{-1}.

These results indicate that, strictly in terms of numerical agreement with the experimental data, the PFO model provides slightly lower errors for *O. anthropi*, whereas the PSO model has smaller errors for *C. metallidurans*. However, both models achieve high R^2 values ($\geq$0.986), suggesting a good overall fit.

For *O. anthropi*, the bioaccumulation process was remarkably efficient and rapid, with most of the americium removed within the first few minutes of contact. The high rate constant k_2 observed for this strain at all concentrations highlights its potential for fast remediation of radioactive waste. For instance, at an initial concentration of 300 Bq mL^{-1}, *O. anthropi* reached a q_e of 1.44 $\times$ 10^{-8} mmol g^{-1}, demonstrating superior performance compared to other microbial systems reported in the literature.

The rapid attainment of equilibrium observed for *O. anthropi* can be attributed to a combination of physical and biological factors. First, fast mass transfer of americium ions in the aqueous medium allows prompt interaction with the bacterial cell surface, which is consistent with observations that diffusion can be a limiting factor in metal sorption processes at low ion concentrations [76]. Although direct evidence of americium-induced aggregation in *O. anthropi* is not available, it is plausible that bacterial cell aggregation could enhance the local density of binding sites, promoting faster bioaccumulation, as observed in other systems where aggregation increases the effective contact between cells and solutes [77]. For *C. metallidurans*, the bioaccumulation process was slightly slower but still highly effective. This bacterium achieved near-complete removal (99.6%) of americium within 6 h of contact. Although its k_2 values were lower than those of *O. anthropi*, the q_e were comparable, indicating that both strains exhibit similar potential for americium uptake despite differences in kinetic rates.

The findings indicate that understanding the kinetic behavior is critical for optimizing the operational parameters of bioaccumulation systems. Factors such as contact time, initial concentration, and bacterial loading can significantly influence the efficiency and scalability of the process.

4. Conclusions

This study demonstrates the promising potential of *C. metallidurans* and *O. anthropi* for the bioremediation of aqueous solutions contaminated with ^{241}Am. Both strains exhibited high uptake efficiencies and rapid removal kinetics, with *O. anthropi* showing exceptional radiotolerance and nearly complete removal within minutes. The kinetic profiles suggest chemisorption as the dominant mechanism for americium uptake.

These results support the feasibility of using metabolically active bacterial biomass in low-energy, biologically based strategies for radioactive waste treatment. Importantly, the goal is not desorption or metal recovery, but rather safe immobilization: once saturated, the biomass can be incorporated into solid matrices such as cement or geopolymers for long-term containment of radionuclides.

Future work should explore the performance of these strains in real or complex waste matrices, including multi-metal systems and organic contaminants, to validate their applicability under practical environmental and industrial conditions.

Supplementary Materials: The following supporting information can be downloaded at: https://www.mdpi.com/article/10.3390/appliedchem5040034/s1, Text S1: Calculation of the ionic strength; Text S2: Calculation of the error metrics [78]; Table S1: TSM Medium Composition; Table S2: Composition of the 10× trace element solution (TES); Table S3: Ionic strength of TSM medium.

Author Contributions: Conceptualization, T.R.d.B. and J.T.M.; Data curation, T.R.d.B.; Formal analysis, L.G.d.A. and T.R.d.B.; Funding acquisition, T.R.d.B. and J.T.M.; Investigation, L.G.d.A. and T.R.d.B.; Methodology, T.R.d.B. and J.T.M.; Project administration, J.T.M.; Resources, J.T.M.; Supervision, E.A.d.S. and J.T.M.; Validation, Leandro de Araujo, T.R.d.B. and R.L.S.C.; Writing—original draft, L.G.d.A.; Writing—review and editing, R.L.S.C., S.N.G., E.A.d.S. and J.T.M. All authors have read and agreed to the published version of the manuscript.

Funding: This research received no external funding.

Institutional Review Board Statement: Not applicable.

Informed Consent Statement: Not applicable.

Data Availability Statement: Data will be made available on request.

Acknowledgments: This study was supported by the Nuclear and Energy Research Institute, the Brazilian National Nuclear Energy Commission and the Brazilian National Council for Scientific and Technological Development.

Conflicts of Interest: The authors declare no conflicts of interest.

Abbreviations

The following abbreviations are used in this manuscript:

PFO	Pseudo-first-order
PSO	Pseudo-second-order
RND	Resistance-nodulation-division
MIC	Minimal inhibitory concentration
TSM	Tris Salt Medium
OD	Optical density
LD-50	Lethal dose for 50%

References

1. Taylor, D. Gut Transfer of Environmental Plutonium and Americium. *Lancet* **1986**, *327*, 611. [CrossRef] [PubMed]
2. Eckerman, K.; Harrison, J.; Menzel, H.-G. *Compendium of Dose Coefficients Based on ICRP Publication 60*; Elsevier: Oxford, UK, 2012; ISBN 978-1-4557-5430-4.

3. Liu, N.; Luo, S.; Yang, Y.; Zhang, T.; Jin, J.; Liao, J. Biosorption of Americium-241 by *Saccharomyces cerevisiae*. *J. Radioanal. Nucl. Chem.* **2002**, *252*, 187–191. [CrossRef]
4. US Environmental Protection Agency (USEPA). National Primary Drinking Water Regulations; Radionuclides; Final Rule. *Fed. Regist.* **2000**, *65*, 76708.
5. Al-Attar, L.; Dyer, A.; Harjula, R. Uptake of Radionuclides on Microporous and Layered Ion Exchange Materials. *J. Mater. Chem.* **2003**, *13*, 2963. [CrossRef]
6. Pérez-Conesa, S.; Martínez, J.M.; Pappalardo, R.R.; Sánchez Marcos, E. Extracting the Americyl Hydration from an Americium Cationic Mixture in Solution: A Combined X-Ray Absorption Spectroscopy and Molecular Dynamics Study. *Inorg. Chem.* **2018**, *57*, 8089–8097. [CrossRef]
7. Kegl, T.; Košak, A.; Lobnik, A.; Novak, Z.; Kralj, A.K.; Ban, I. Adsorption of Rare Earth Metals from Wastewater by Nanomaterials: A Review. *J. Hazard. Mater.* **2020**, *386*, 121632. [CrossRef] [PubMed]
8. Deblonde, G.J.-P.; Mattocks, J.A.; Wang, H.; Gale, E.M.; Kersting, A.B.; Zavarin, M.; Cotruvo, J.A. Characterization of Americium and Curium Complexes with the Protein Lanmodulin: A Potential Macromolecular Mechanism for Actinide Mobility in the Environment. *J. Am. Chem. Soc.* **2021**, *143*, 15769–15783. [CrossRef]
9. Volesky, B. Detoxification of Metal-Bearing Effluents: Biosorption for the next Century. *Hydrometallurgy* **2001**, *59*, 203–216. [CrossRef]
10. Kmak, K.N.; Despotopulos, J.D.; Huynh, T.L.; Kerlin, W.M. TALSPEAK-Based Separation of the Trivalent Actinides from Rare Earth Elements Using LN Resin. *J. Radioanal. Nucl. Chem.* **2025**, *334*, 2407–2415. [CrossRef]
11. Kolesar, F.; Van Hecke, K.; Zsabka, P.; Verguts, K.; Binnemans, K.; Cardinaels, T. Separation of Americium from Highly Active Raffinates by an Innovative Variant of the AmSel Process Based on the Ionic Liquid Aliquat-336 Nitrate. *RSC Adv.* **2023**, *13*, 36322–36336. [CrossRef]
12. Vidanov, V.L.; Shadrin, A.Y.; Tkachenko, L.I.; Kenf, E.V.; Parabin, P.V.; Shirokov, S.S. Separation of Americium and Curium for Transmutation in the Fast Neutron Reactor. *Nucl. Eng. Des.* **2021**, *385*, 111434. [CrossRef]
13. Mincher, B.J.; Law, J.D.; Goff, G.S.; Moyer, B.A.; Burns, J.D.; Lumetta, G.J.; Sinkov, S.I.; Shehee, T.C.; Hobbs, D.T. *Higher Americium Oxidation State Research Roadmap*; Idaho National Lab. (INL): Idaho Falls, ID, USA, 2015.
14. Dursun, A.Y.; Uslu, G.; Tepe, O.; Cuci, Y.; Ekiz, H.I. A Comparative Investigation on the Bioaccumulation of Heavy Metal Ions by Growing *Rhizopus arrhizus* and *Aspergillus niger*. *Biochem. Eng. J.* **2003**, *15*, 87–92. [CrossRef]
15. Kaduková, J.; Virčíková, E. Comparison of Differences between Copper Bioaccumulation and Biosorption. *Environ. Int.* **2005**, *31*, 227–232. [CrossRef]
16. Al-Saraj, M.; Abdel-Latif, M.S.; El-Nahal, I.; Baraka, R. Bioaccumulation of Some Hazardous Metals by Sol–Gel Entrapped Microorganisms. *J. Non-Cryst. Solids* **1999**, *248*, 137–140. [CrossRef]
17. Velásquez, L.; Dussan, J. Biosorption and Bioaccumulation of Heavy Metals on Dead and Living Biomass of *Bacillus sphaericus*. *J. Hazard. Mater.* **2009**, *167*, 713–716. [CrossRef] [PubMed]
18. Ayele, A.; Haile, S.; Alemu, D.; Kamaraj, M. Comparative Utilization of Dead and Live Fungal Biomass for the Removal of Heavy Metal: A Concise Review. *Sci. World J.* **2021**, 5588111. [CrossRef]
19. Spain, O.; Plöhn, M.; Funk, C. The Cell Wall of Green Microalgae and Its Role in Heavy Metal Removal. *Physiol. Plant.* **2021**, *173*, 526–535. [CrossRef]
20. Chang, J.-S.; Law, R.; Chang, C.-C. Biosorption of Lead, Copper and Cadmium by Biomass of *Pseudomonas aeruginosa* PU21. *Water Res.* **1997**, *31*, 1651–1658. [CrossRef]
21. Liu, F.; Hua, S.; Xia, F.; Hu, B. Efficient Extraction of Radionuclides with MXenes/Persimmon Tannin Functionalized Cellulose Nanofibers: Performance and Mechanism. *Appl. Surf. Sci.* **2023**, *609*, 155254. [CrossRef]
22. Ioannidis, I.; Pashalidis, I.; Raptopoulos, G.; Paraskevopoulou, P. Radioactivity/Radionuclide (U-232 and Am-241) Removal from Waters by Polyurea-Crosslinked Alginate Aerogels in the Sub-Picomolar Concentration Range. *Gels* **2023**, *9*, 211. [CrossRef]
23. de Araujo, L.G.; de Borba, T.R.; de Pádua Ferreira, R.V.; Canevesi, R.L.S.; da Silva, E.A.; Dellamano, J.C.; Marumo, J.T.; Araujo, L.G.d.; Borba, T.R.d.; Ferreira, R.V.d.P.; et al. Use of Calcium Alginate Beads and *Saccharomyces cerevisiae* for Biosorption of ^{241}Am. *J. Environ. Radioact.* **2020**, *223–224*, 106399. [CrossRef]
24. Zhou, L.; Dong, F.; Dai, Q.; Liu, M.; Zhang, W.; Zhang, Y. Transformation of Radionuclide Occurrence State in Uranium and Strontium Recycling by *Saccharomyces cerevisiae*. *J. Radioanal. Nucl. Chem.* **2022**, *331*, 2621–2629. [CrossRef]
25. Hupian, M.; Rosskopfová, O.; Viglašová, E.; Vyhnáleková, S.; Daňo, M.; Švajdlenková, H.; Galamboš, M. Investigation of the Adsorptive Properties of Filamentous Fungus *Aspergillus niger* in the Removal of ^{85}Sr and ^{99m}Tc from Aqueous Solutions. *J. Radioanal. Nucl. Chem.* **2025**, *334*, 6849–6862. [CrossRef]
26. Liu, L.; Chen, J.; Liu, F.; Song, W.; Sun, Y. Bioaccumulation of Uranium by *Candida Utilis*: Investigated by Water Chemistry and Biological Effects. *Environ. Res.* **2021**, *194*, 110691. [CrossRef] [PubMed]

27. Monchy, S.; Benotmane, M.A.; Janssen, P.; Vallaeys, T.; Taghavi, S.; van der Lelie, D.; Mergeay, M. Plasmids pMOL28 and pMOL30 of *Cupriavidus metallidurans* Are Specialized in the Maximal Viable Response to Heavy Metals. *J. Bacteriol.* **2007**, *189*, 7417–7425. [CrossRef]
28. Janssen, P.J.; Van Houdt, R.; Moors, H.; Monsieurs, P.; Morin, N.; Michaux, A.; Benotmane, M.A.; Leys, N.; Vallaeys, T.; Lapidus, A.; et al. The Complete Genome Sequence of *Cupriavidus metallidurans* Strain CH34, a Master Survivalist in Harsh and Anthropogenic Environments. *PLoS ONE* **2010**, *5*, e10433. [CrossRef]
29. von Rozycki, T.; Nies, D.H. *Cupriavidus metallidurans*: Evolution of a Metal-Resistant Bacterium. *Antonie Van Leeuwenhoek* **2009**, *96*, 115. [CrossRef]
30. Millacura, F.A.; Janssen, P.J.; Monsieurs, P.; Janssen, A.; Provoost, A.; Van Houdt, R.; Rojas, L.A. Unintentional Genomic Changes Endow *Cupriavidus metallidurans* with an Augmented Heavy-Metal Resistance. *Genes* **2018**, *9*, 551. [CrossRef]
31. Große, C.; Kohl, T.A.; Niemann, S.; Herzberg, M.; Nies, D.H. Loss of Mobile Genomic Islands in Metal-Resistant, Hydrogen-Oxidizing *Cupriavidus metallidurans*. *Appl. Environ. Microbiol.* **2022**, *88*, e02048-21. [CrossRef]
32. Herzberg, M.; Bauer, L.; Kirsten, A.; Nies, D.H. Interplay between Seven Secondary Metal Uptake Systems Is Required for Full Metal Resistance of *Cupriavidus metallidurans*. *Metallomics* **2016**, *8*, 313–326. [CrossRef]
33. Colliard, I.; Deblonde, G.J.-P. Polyoxometalate Ligands Reveal Different Coordination Chemistries Among Lanthanides and Heavy Actinides. *JACS Au* **2024**, *4*, 2503–2513. [CrossRef] [PubMed]
34. Li, X.; Feng, J.; Zhu, X.; Zhu, F.; Ke, W.; Huang, Y.; Wu, C.; Xu, X.; Guo, J.; Xue, S. Organic Acid Release and Microbial Community Assembly Driven by Phosphate-Solubilizing Bacteria Enhance Pb, Cd, and As Immobilization in Soils Remediated with Iron-Doped Hydroxyapatite. *J. Hazard. Mater.* **2025**, *488*, 137340. [CrossRef]
35. Wei, W.; Liu, X.; Sun, P.; Wang, X.; Zhu, H.; Hong, M.; Mao, Z.-W.; Zhao, J. Simple Whole-Cell Biodetection and Bioremediation of Heavy Metals Based on an Engineered Lead-Specific Operon. *Environ. Sci. Technol.* **2014**, *48*, 3363–3371. [CrossRef]
36. Rivas-Castillo, A.M.; Monges-Rojas, T.L.; Rojas-Avelizapa, N.G. Specificity of Mo and V Removal from a Spent Catalyst by *Cupriavidus metallidurans* CH34. *Waste Biomass Valorization* **2019**, *10*, 1037–1042. [CrossRef]
37. Ali, M.M.; Provoost, A.; Maertens, L.; Leys, N.; Monsieurs, P.; Charlier, D.; Houdt, R.V. Genomic and Transcriptomic Changes That Mediate Increased Platinum Resistance in *Cupriavidus metallidurans*. *Genes* **2019**, *10*, 63. [CrossRef]
38. Bütof, L.; Große, C.; Lilie, H.; Herzberg, M.; Nies, D.H. Interplay between the Zur Regulon Components and Metal Resistance in *Cupriavidus metallidurans*. *J. Bacteriol.* **2019**, *201*, e00192-19. [CrossRef]
39. Millacura, F.A.; Cardenas, F.; Mendez, V.; Seeger, M.; Rojas, L.A. Degradation of Benzene by the Heavy-Metal Resistant Bacterium *Cupriavidus metallidurans* CH34 Reveals Its Catabolic Potential for Aromatic Compounds. *bioRxiv* **2017**, 164517. [CrossRef]
40. Shamim, S.; Rehman, A.; Qazi, M.H. Swimming, Swarming, Twitching, and Chemotactic Responses of *Cupriavidus metallidurans* CH34 and *Pseudomonas putida* Mt2 in the Presence of Cadmium. *Arch. Environ. Contam. Toxicol.* **2014**, *66*, 407–414. [CrossRef] [PubMed]
41. Llorens, I.; Untereiner, G.; Jaillard, D.; Gouget, B.; Chapon, V.; Carriere, M. Uranium Interaction with Two Multi-Resistant Environmental Bacteria: *Cupriavidus metallidurans* CH34 and *Rhodopseudomonas palustris*. *PLoS ONE* **2012**, *7*, e51783. [CrossRef]
42. Seleem, M.N.; Ali, M.; Boyle, S.M.; Mukhopadhyay, B.; Witonsky, S.G.; Schurig, G.G.; Sriranganathan, N. Establishment of a Gene Expression System in *Ochrobactrum anthropi*. *Appl. Environ. Microbiol.* **2006**, *72*, 6833–6836. [CrossRef]
43. Ozdemir, G.; Ozturk, T.; Ceyhan, N.; Isler, R.; Cosar, T. Heavy Metal Biosorption by Biomass of *Ochrobactrum anthropi* Producing Exopolysaccharide in Activated Sludge. *Bioresour. Technol.* **2003**, *90*, 71–74. [CrossRef]
44. Cheng, Y.; Yan, F.; Huang, F.; Chu, W.; Pan, D.; Chen, Z.; Zheng, J.; Yu, M.; Lin, Z.; Wu, Z. Bioremediation of Cr (VI) and Immobilization as Cr (III) by *Ochrobactrum anthropi*. *Environ. Sci. Technol.* **2010**, *44*, 6357–6363. [CrossRef]
45. Li, B.; Pan, D.; Zheng, J.; Cheng, Y.; Ma, X.; Huang, F.; Lin, Z. Microscopic Investigations of the Cr(VI) Uptake Mechanism of Living *Ochrobactrum anthropi*. *Langmuir* **2008**, *24*, 9630–9635. [CrossRef]
46. de Pádua Ferreira, R.V.; Sakata, S.K.; Isiki, V.L.K.; Miyamoto, H.; Bellini, M.H.; de Lima, L.F.C.P.; Marumo, J.T. Influence of Americium-241 on the Microbial Population and Biodegradation of Organic Waste. *Environ. Chem. Lett.* **2011**, *9*, 209–216. [CrossRef]
47. Mazhar, S.H.; Herzberg, M.; Ben Fekih, I.; Zhang, C.; Bello, S.K.; Li, Y.P.; Su, J.; Xu, J.; Feng, R.; Zhou, S.; et al. Comparative Insights into the Complete Genome Sequence of Highly Metal Resistant *Cupriavidus metallidurans* Strain BS1 Isolated from a Gold–Copper Mine. *Front. Microbiol.* **2020**, *11*, 47. [CrossRef] [PubMed]
48. Maertens, L.; Leys, N.; Matroule, J.-Y.; Van Houdt, R. The Transcriptomic Landscape of *Cupriavidus metallidurans* CH34 Acutely Exposed to Copper. *Genes* **2020**, *11*, 1049. [CrossRef]
49. Taghavi, S.; Lesaulnier, C.; Monchy, S.; Wattiez, R.; Mergeay, M.; Van Der Lelie, D. Lead(II) Resistance in *Cupriavidus metallidurans* CH34: Interplay between Plasmid and Chromosomally-Located Functions. *Antonie Van Leeuwenhoek* **2009**, *96*, 171–182. [CrossRef] [PubMed]
50. Rogiers, T.; Merroun, M.L.; Williamson, A.; Leys, N.; Houdt, R.V.; Boon, N.; Mijnendonckx, K. *Cupriavidus metallidurans* NA4 Actively Forms Polyhydroxybutyrate-Associated Uranium-Phosphate Precipitates. *J. Hazard. Mater.* **2022**, *421*, 126737. [CrossRef]

51. Alviz-Gazitua, P.; Durán, R.E.; Millacura, F.A.; Cárdenas, F.; Rojas, L.A.; Seeger, M. *Cupriavidus metallidurans* CH34 Possesses Aromatic Catabolic Versatility and Degrades Benzene in the Presence of Mercury and Cadmium. *Microorganisms* **2022**, *10*, 484. [CrossRef]
52. Große, C.; Scherer, J.; Schleuder, G.; Nies, D.H. Interplay between Two-Component Regulatory Systems Is Involved in Control of *Cupriavidus metallidurans* Metal Resistance Genes. *J. Bacteriol.* **2023**, *205*, e00343-22. [CrossRef]
53. Cheng, H.; Yuan, M.; Zeng, Q.; Zhou, H.; Zhan, W.; Chen, H.; Mao, Z.; Wang, Y. Efficient Reduction of Reactive Black 5 and Cr(VI) by a Newly Isolated Bacterium of *Ochrobactrum anthropi*. *J. Hazard. Mater.* **2021**, *406*, 124641. [CrossRef]
54. Villagrasa, E.; Palet, C.; López-Gómez, I.; Gutiérrez, D.; Esteve, I.; Sánchez-Chardi, A.; Solé, A. Cellular Strategies against Metal Exposure and Metal Localization Patterns Linked to Phosphorus Pathways in *Ochrobactrum anthropi* DE2010. *J. Hazard. Mater.* **2021**, *402*, 123808. [CrossRef]
55. Talwar, M.P.; Mulla, S.I.; Ninnekar, H.Z. Biodegradation of Organophosphate Pesticide Quinalphos by *Ochrobactrum* sp. Strain HZM. *J. Appl. Microbiol.* **2014**, *117*, 1283–1292. [CrossRef] [PubMed]
56. Rinanti, A.; Nainggolan, I.J. Petroleum Residues Degradation in Laboratory-Scale by *Rhizosphere* Bacteria Isolated from the Mangrove Ecosystem. *IOP Conf. Ser. Earth Environ. Sci.* **2018**, *106*, 012100. [CrossRef]
57. Mergeay, M.; Nies, D.; Schlegel, H.G.; Gerits, J.; Charles, P.; Van Gijsegem, F. *Alcaligenes eutrophus* CH34 Is a Facultative Chemolithotroph with Plasmid-Bound Resistance to Heavy Metals. *J. Bacteriol.* **1985**, *162*, 328–334. [CrossRef] [PubMed]
58. CLSI. *Metodologia Dos Testes de Sensibilidade a Agentes Antimicrobianos Por Diluição Para Bactéria de Crescimento Aeróbico: Norma Aprovada-Sexta Edição*; CLSI: Wayne, PA, USA, 2003; Volume 23, ISBN 1-56238-486-4.
59. Borkowski, M.; Lucchini, J.-F.; Richmann, M.; Reed, D. *Actinide (III) Solubility in WIPP Brine: Data Summary and Recommendations (No. LA-14360)*; Los Alamos National Laboratory (LANL): Los Alamos, NM, USA, 2009; p. 966984.
60. Takeda, S. *Analysis of Americium, Plutonium and Technetium Solubility in Groundwater*; Japan Atomic Energy Research Inst.: Tokyo, Japan, 1999.
61. Madigan, M.T.; Martinko, J.M.; Bender, K.S.; Buckley, D.H.; Stahl, D.A. *Microbiologia de Brock-14ª Edição*; Artmed Editora: Porto Alegre, Brazil, 2016; ISBN 85-8271-298-7.
62. Jepras, R.I.; Carter, J.; Pearson, S.C.; Paul, F.E.; Wilkinson, M.J. Development of a Robust Flow Cytometric Assay for Determining Numbers of Viable Bacteria. *Appl. Environ. Microbiol.* **1995**, *61*, 2696–2701. [CrossRef] [PubMed]
63. Perrier, T.; Martin-Garin, A.; Morello, M. Am-241 Remobilization in a Calcareous Soil under Simplified Rhizospheric Conditions Studied by Column Experiments. *J. Environ. Radioact.* **2005**, *79*, 205–221. [CrossRef]
64. Lagergren, S.; Lagergren, S.; Lagergren, S.Y.; Sven, K. Zur Theorie der Sogenannten Adsorption Gelöster Stoffe. *Colloid Polym. Sci.* **1898**, *24*, 15. [CrossRef]
65. Ho, Y.S.; McKay, G. Pseudo-Second Order Model for Sorption Processes. *Process Biochem.* **1999**, *34*, 451–465. [CrossRef]
66. Matsumura, T.; Usuda, S. Applicability of Insoluble Tannin to Treatment of Waste Containing Americium. *J. Alloys Compd.* **1998**, *271*, 244–247. [CrossRef]
67. Das, S.K.; Kedari, C.S.; Shinde, S.S.; Ghosh, S.; Jambunathan, U. Performance of Immobilized *Saccharomyces cerevisiae* in the Removal of Long Lived Radionuclides from Aqueous Nitrate Solutions. *J. Radioanal. Nucl. Chem.* **2002**, *253*, 235–240. [CrossRef]
68. Dhami, P.S.; Kannan, R.; Naik, P.W.; Gopalakrishnan, V.; Ramanujam, A.; Salvi, N.A. Biosorption of Americium Using Biomasses of Various *Rhizopus* Species. *Biotechnol. Lett.* **2002**, *24*, 885–889. [CrossRef]
69. Liao, J.; Yang, Y.; Luo, S.; Liu, N.; Jin, J.; Zhang, T.; Zhao, P. Biosorption of Americium-241 by Immobilized *Rhizopus arrihizus*. *Appl. Radiat. Isot.* **2004**, *60*, 1–5. [CrossRef]
70. Luo, B.S.; Liu, N.; Yang, Y.; Zhang, T.; Jin, J.; Liao, J. Biosorption of Americium-241 by *Candida* sp. *Radiochim. Acta* **2003**, *91*, 315–318.
71. Takenaka, Y.; Saito, T.; Nagasaki, S.; Tanaka, S.; Kozai, N.; Ohnuki, T. Metal Sorption to *Pseudomonas Fluorescens*: Influence of pH, Ionic Strength and Metal Concentrations. *Geomicrobiol. J.* **2007**, *24*, 205–210. [CrossRef]
72. Luk'yanova, E.A.; Zakharova, E.V.; Konstantinova, L.I.; Nazina, T.N. Sorption of Radionuclides by Microorganisms from a Deep Repository of Liquid Low-Level Waste. *Radiochemistry* **2008**, *50*, 85–90. [CrossRef]
73. Bustamante, P.; Teyssié, J.-L.; Fowler, S.W.; Warnau, M. Assessment of the Exposure Pathway in the Uptake and Distribution of Americium and Cesium in Cuttlefish (*Sepia officinalis*) at Different Stages of Its Life Cycle. *J. Exp. Mar. Biol. Ecol.* **2006**, *331*, 198–207. [CrossRef]
74. Bolsunovsky, A.; Zotina, T.; Bondareva, L. Accumulation and Release of ^{241}Am by a Macrophyte of the Yenisei River (*Elodea canadensis*). *J. Environ. Radioact.* **2005**, *81*, 33–46. [CrossRef] [PubMed]
75. Jeffree, R.A.; Markich, S.J.; Oberhaensli, F.; Teyssie, J.-L. Biokinetics of Americium-241 in the Euryhaline Diamond Sturgeon *Acipenser gueldenstaedtii* Following Its Uptake from Water or Food. *J. Environ. Radioact.* **2024**, *278*, 107503. [CrossRef] [PubMed]
76. Ioannidis, I.; Xenofontos, A.; Anastopoulos, I.; Pashalidis, I. Americium Sorption by Microplastics in Aqueous Solutions. *Coatings* **2022**, *12*, 1452. [CrossRef]

77. Tavaddod, S.; Dawson, A.; Allen, R.J. Bacterial Aggregation Triggered by Low-Level Antibiotic-Mediated Lysis. *npj Biofilms Microbiomes* **2024**, *10*, 90. [CrossRef] [PubMed]
78. Cao, X.; Luo, W.; Liu, H. A Prediction Model for CO_2/CO Adsorption Performance on Binary Alloys Based on Machine Learning. *RSC Adv.* **2024**, *14*, 12235–12246. [CrossRef] [PubMed]

Disclaimer/Publisher's Note: The statements, opinions and data contained in all publications are solely those of the individual author(s) and contributor(s) and not of MDPI and/or the editor(s). MDPI and/or the editor(s) disclaim responsibility for any injury to people or property resulting from any ideas, methods, instructions or products referred to in the content.